SEMARAK ILMU PUBLISHING

Journal of Advanced Research in Fluid Mechanics and Thermal Sciences

Journal homepage:
https://semarakilmu.com.my/journals/index.php/fluid_mechanics_thermal_sciences/index
ISSN: 2289-7879

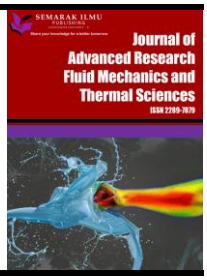

Numerical Simulation of the Fin Impact on the Cooling of the Shell of a Rotary Kiln

Mohammed Bouhafs[1], Abed Meghdir[1], Abdelaziz Adjeloua[2], Houari Ameur[3,*]

[1] Department of Electromechanics, Institute of Maintenance and Industrial Safety, University of Oran 2, Oran, Algeria
[2] Laboratory of Composites Structures and Innovative Materials (LCSIM), Mechanical Engineering Faculty, USTO-MB Oran, P.O. Box 1505 El-M'Naouar, Oran, Algeria
[3] Department of Technology, University Centre of Naama, P.O. Box 66, 45000, Algeria

ARTICLE INFO

Article history:
Received 20 October 2022
Received in revised form 27 January 2023
Accepted 3 February 2023
Available online 21 February 2023

Keywords:
Rotary kiln; shell; natural convection; Nusselt number; finite volumes

ABSTRACT

This work consists of a numerical study of a thermally stressed rotary kiln shell part in a cement plant. The numerical simulations are performed by using the finite volume method for the discretization and the simple algorithm for resolution. The velocity air injection, its temperature, and the kiln rotational velocity are the main parameters under investigation. The distribution of temperature, velocity, and pressure, as well as the evolution of the Nusselt number are determined. In the second step of this study, fins are inserted on the shell to examine their effect on cooling. The results analysis shows that the insertion of fins to the shell has a significant influence on the decrease in temperature of the shell's external surface. The study shows that this decrease in temperature depends significantly on the air injection rate, not on its temperature, and a bit less on the rotating velocity of the kiln. To avoid overloading our equipment (weight of the shell), only four fins distributed around the kiln are added to explore their effect.

1. Introduction

The cement industry has experienced a gradual improvement in recent years with the increase in the number of cement production lines. The rotary kiln is the main equipment of a cement plant, as it is used for firing basic materials for the production of clinker. It consists of a steel tube coated with refractory brick. The tube is slightly inclined (1 to 4 degrees) and rotates between 0.5 and 5 rpm. The rotary kiln is of great importance in the field of cement production. It represents the most thermally stressed component, and the resolution of problems associated with this phenomenon leads to a better performance of the kiln. To address these issues, we began with the study of the thermal behaviour of the rotary kiln shell. To improve the evacuation of heat flow and to reduce the temperature of the shell, we worked on various system parameters, such as the rotational velocity of the kiln and the rate of air injection.

* *Corresponding author.*
E-mail address: ameur.houari@cuniv-naama.dz; houari_ameur@yahoo.fr

https://doi.org/10.37934/arfmts.103.2.6884

Due to the temperature difference between the inner surface of the rotary kiln and that of the surrounding air, there will be a large heat transfer between these two media. Many works have studied these thermal transfers. We shall mention those of Mirhosseini *et al.,* [1], who studied the effect of an absorber placed around the rotary kiln to allow the recovery of part of this heat quantity for other applications. Shahin *et al.,* [2] analyzed the thermal energy of a cement plant rotating kiln. They found that an increase of 10 minutes residence time of the materials inside the rotary kiln can reduce fuel consumption. Atmaca and Yumrutas [3] calculated the heat transfer coefficients of the different heat transfer modes. Next, several system parameters were analysed to deduce the mathematical relationship between these parameters and the requirements of the heat recovery system. Acharya and Dash [4] studied the heat transfer by natural convection on a short and long, solid and hollow horizontal cylinder, suspended in the air and placed on the ground. By using different CFD models, Gaurav and Khanam [5] discussed the effects of varying input parameters on the temperature profile of the rotary kiln. The obtained results agreed with those of the operation. Liu *et al.,* [6] gave a two-fluid approach, and various heat transfer models were applied to a two-dimensional cross-section of a rotary kiln. The results found were compared with the available experimental data. They found that the significant factors affecting fluid temperature distribution are the initial temperature of the gas and the kiln rotational velocity. Li *et al.,* [7] deduced a three-dimensional digital model of the rotary kiln configured according to the finite element method. They observed that the temperature of the outer wall of the rotary kiln had an approximately linear relationship with the crusting thickness of the kiln. Sak *et al.,* [8] studied the effect of turbulence intensity and convection rate on a heated cylinder, with a Reynolds number of 27,700, for the transversal airflow and a cylinder diameter between 0.50 and 1.47 m. Sanitjai and Goldstein [9] brought separate empirical correlations of Nusselt number for the region of the laminar boundary layer, re-adhesion of the shear layer region, and the periodic vortex flow region. For the mean Nusselt, an empirical correlation was suggested and compared to previous correlations considering all regimes. Nakamura and Igarashi [10] studied experimentally the heat transfer from a cylinder, for *Re* values included between 70 and 30,000, and between 3000 and 15000. Scholten and Murray [11] reported the experimental results of a heat transfer on a cylinder for a low turbulence range. Then, they studied a higher turbulence range of the free flow. Zukauskas and Ziugzda [12] conducted experimentation on the heat transfer by convection through a cylinder. They showed correlations for a wide range of Prandtl and Reynolds numbers. Sarma and Sukhatme [13] performed measurements of thermal transfer on a horizontal circular cylinder undergoing a transversal airflow by considering two separate cases, i.e., forced convection and mixed convection. The study assumed the following conditions: a constant flux density, Reynolds numbers varying from 500 to 4700, the Grashof numbers ranging from 0.8×107 to 3.3×107, and the variation of the incidental turbulence intensity between 0.5 and 20%. Jain & Goel [14] studied the unstable forced laminar convection of a circular cylinder by solving the Navier-Stokes equations and energy for a flow of an incompressible and unsteady fluid. Using the finite difference method and varying the Reynolds number of 100 to 200, they determined a temperature field around the cylinder and the variation in Nusselt and Strouhal numbers. Schmidt and Wenner [15] produced work dealing with heat transfer to a cylinder. Numerous experimental results investigating heat transfer and the characteristics of hydrodynamics cylinders were presented. Elfaghi *et al.,* [16] presented a numerical simulation of computational fluid dynamics (CFD). They highlighted the heat transfer by forced convection of Al_2O_3 nanofluids, in a circular tube with a constant heat flux. They studied the variations of the convective heat transfer coefficient, the Nusselt number and the friction factor as a function of the Reynolds number and the volume fraction of the particles. Kanafiah *et al.,* [17] studied the flow of a Brinkman viscoelastic fluid, in a horizontal circular cylinder with the influence of the convective boundary condition (CBC). They

highlighted the problem of combined convective stationary transport. The aim of the study realized by Shafie *et al.,* [18] is to numerically illustrate the impact of viscous dissipation on the two-dimensional flow of stable mixed convection through a horizontal cylinder in a viscoelastic nanofluid. The parameters highlighted for a variation of the Eckert number are, the velocity, the temperature, the coefficient of internal friction as well as the coefficient of heat transfer. Mujumdar *et al.,* [19] presented an integrated mathematical model based on reaction engineering for the formation of clinker in the cement industry. This model integrated the preheater, the calciner, the rotary kiln and the cooler, in order to create an integrated simulator. This allowed them to model complex heat transfers and reactions in a rotary kiln. Mujumdar and Ranade [20] numerically simulated a one-dimensional model of the processes occurring in a bed of material feeding a cement kiln. They studied the effect of the main operating and design parameters in order to reduce its energy consumption. They also explored the possibility of manipulating the temperature profile in the kiln for the same purpose.

The work consists of a comparative study of the external temperature of the shell of a rotary kiln of cement factory without and with fin. With other explanation, in this case of figure is that the installation of fin can reduce this temperature, which will add a plus for the preservation of the shell.

2. Calculation Domain

The study was done on a 3.6 m diameter rotary kiln. Regarding the length, only the kiln section was taken, as it is the most thermally loaded. The kiln temperature (*T*), reached in these positions is 500 °C (773 K), which could damage the kiln shell. The outside temperature T_∞ is taken equal to 5 °C (278 K). The rotational velocity of the kiln is 5 rpm; the rate of injection of air blowing on the kiln is 5.85 m/s. The rotational velocity of the rotary kiln is a very important parameter, because it allows us to have an ideal firing of our clinker with the material feed rate. During operation, the rotational velocity of the oven varies between 1 to 5 rpm. For our simulation, we took 5 rpm as the value of the rotational velocity, which is the most used cruising velocity for optimum material flow. Figure 1 present the computational domain of the studied model, and the boundary conditions used for our simulation. In our case study, which is a rotary cement kiln, where it operates at high temperatures exceeding 1400 °C (internal temperature of the kiln) and around 500°C (external temperature of the shell). For this temperature, we took the highest crack temperature, which is 500 °C and located in the most thermally stressed part, which is the cooking zone. It is taken constant and uniform. Thus, to allow a combination between the different heat transfer modes at high Reynolds and Rayleigh numbers, the flow is considered to be mainly turbulent. The center of the kiln is placed 20 D upstream and 40 D downstream with respect to the X axis, while with respect to the Y axis, a range of 40 D has been taken, divided into two equal parts upstream and downstream. This computational domain will allow us to avoid the effect of a boundary condition on the characteristics of fluid flow and heat transfer. At the entrance to the domain, Air is considered as the working fluid, with velocity U_∞ and a temperature T_∞ are imposed. These initial conditions and computational domain are those of the paper of our validation case Mirhosseini *et al.,* [1].

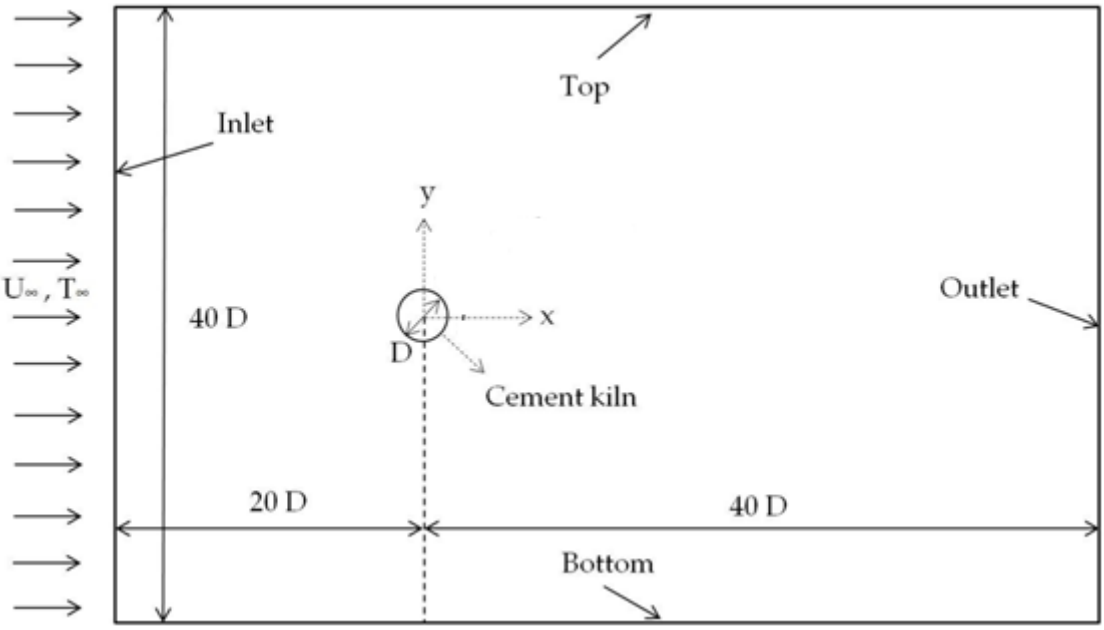

Fig. 1. Rotary kiln calculation domain [1]

3. Modelling of Convective Transfer

Our study consists of an approach of a flow around a horizontal cylinder with a wall at high temperature. For this, it is necessary to quote the adequate formulation for this case. The resolution of the equations governing this flow is done by the K-ω-SST model of the ANSYS-CFX code, the comparison of the results of which constitutes the essential objective of this work. By adopting the SST model simulates the heat transfer of this flow. The Navier Stocks equations considered for this incompressible fluid are [21,22]

Continuity equation

$$\frac{\partial U_j}{\partial x_j} = 0 \tag{1}$$

Momentum Transport Equations

$$\rho U_j \frac{\partial}{\partial x_j}(U_i) = -\frac{\partial P}{\partial x_j} + \mu \frac{\partial^2 u_i}{\partial x_j^2} + \underbrace{\frac{\partial}{\partial x_j}\left(-\rho\overline{u_i' u_j'}\right)}_{\text{Contraintes de Reynolds}} + \rho g_i \tag{2}$$

Energy equation

$$\frac{\partial}{\partial x_j}\left(\rho U_j T\right) = \frac{\lambda}{C_p}\frac{\partial^2 T}{\partial x_j^2} + \frac{\partial}{\partial x_j}\left(-\overline{\rho u_j' t_p'}\right) \tag{3}$$

All these equations can be written in the following general form

$$\underbrace{\frac{\partial(\rho U_j \phi)}{\partial x_j}}_{1} = \underbrace{\frac{\partial}{\partial x_j}\left(\Gamma_\phi \frac{\partial \phi}{\partial x}\right)}_{2} + \underbrace{S_\phi}_{3} \tag{4}$$

Term 1: transport of ϕ by convection.
Term 2: transport of ϕ by diffusion.
Term 3: local production of ϕ.
The SST model has a form similar to the standard $k-\omega$ model [22]

$$\frac{\delta}{\delta x_i}(\rho k u_i) = \frac{\delta}{\delta x_j}\left[\Gamma_k \frac{\delta k}{\delta x_j}\right] + G_k - y_k + S_k \tag{5}$$

$$\frac{\delta}{\delta x_i}(\rho \omega u_i) = \frac{\delta}{\delta x_j}\left[\Gamma_\omega \frac{\delta \omega}{\delta x_j}\right] + G_\omega - y_\omega + \ D_\omega + S_\omega \tag{6}$$

Avec $G_k = -\rho\overline{u_i' u_j'}\frac{\partial u_i}{\partial x_i}$, $G_\omega = \alpha\frac{\omega}{k}G_k$: le terme de production de k,ω respectivement.

The effective diffusivities for the SST model are given by

$$\Gamma_k = \mu + \frac{\pi_t}{\sigma_k} \tag{7}$$

$$\Gamma_\omega = \mu + \frac{\pi_t}{\sigma_\omega} \tag{8}$$

The empirical constants of the SST model are presented in Table 1

Table 1
Value of the constants of the SST model

α_∞^*	α_∞	β_∞^*	R_β	Mt_0	α_1	$\beta_{i,1}$	$\beta_{i,2}$	$\sigma_{k,1}$	$\sigma_{k,2}$	$\sigma_{\omega,1}$	$\sigma_{\omega,2}$
1	0.52	0.09	8	0.25	0.31	0.075	0.0828	1.176	1	2	1.168

This study deals with heat transfer through the laminar regime convection between the steel shell and its external environment. It describes the movement of a fluid due to changes in density as a function of temperature. Thus, there is a coupling between the dynamic and the thermal. For all convection problems, the wall heat exchanges are measured by highlighting the value of the Nu number.

Since our study has an orientation towards heat transfer with the existence of a rectangular fin with a finite end, we give the equation that governs this phenomenon [23]

$$\frac{d}{dx}\left(\lambda A\frac{dT}{dx}\right) - hp(T - T_\infty) = 0 \tag{9}$$

For heat transfer by natural convection, The Nusselt number correlation for the horizontal cylinder with plate fins (Nu) is given by [24]

$$Nu = \left(1 - 0.117N + 0.353\left(\frac{l}{D_e}\right)\right)\left(0.6 + \frac{0.387Ra^{1/6}}{\left(1+(0.559/Pr)^{9/16}\right)^{8/27}}\right)^2 \tag{10}$$

The fin efficiency η, which is written as follows [20]

$$\eta = \frac{(hp\lambda A_c)^{0.5}}{hA_f} \frac{tanh\left(\sqrt{\frac{hp}{\lambda A_c}}l\right)+\left(h/\sqrt{\frac{hp}{\lambda A_c}}\lambda\right)}{1+\left(h/\sqrt{\frac{hp}{\lambda A_c}}\lambda\right)tanh\left(\sqrt{\frac{hp}{\lambda A_c}}l\right)} \quad (11)$$

4. Optimizing the Grid

The quality of our simulation results is closely linked to the model used. The choice of model is contingent on the type of information we want to obtain from the simulation. We carried out three simulations to optimize the grid for reasons of result precisions and computation time. Table 2 shows the three tested grids. We have opted for a refined uniform grid near the wall of the rotary kiln. According to the results, the second grid gives a good optimization compared to the two others.

Table 2
Grid optimization

Nusselt number	Number of elements	Number of nodes
3942	578,185	557,286
4299	843,932	825,648
4300	1,254,234	1,227,695

5. Results and Discussion

A thermal study was performed to derive the various parameters that influence the temperature of the rotary kiln and the evolution of the Nusselt number. For this purpose, we have taken different velocity values, air injection, and kiln rotation. To illustrate our results, a tangential line to the top kiln wall parallel to the *x*-axis was designated as a reference for extracting the results. The results of the simulation were obtained using the algorithm SIMPLE as a solution method.

5.1 Validation

Table 3 shows the values of the average number of Nusselt calculated in our case study and those published by Mirhosseini *et al.,* [1], as well as the percentage difference. The analysis of the results shows that the calculations of our research are very satisfactory. We note that the error in our case of study is evaluated at 3.87% compared to the analytical solution.

Table 3
The average Nusselt number

	Nusselt number	Difference
Analytical solution [1]	4473.2572	----
Numerical solution [1]	3628.71	18.88%
Numerical solution (our study)	4299.95	3.87%

5.2 1st Case "Smooth Cylinder"
5.2.1 Temperature contour

Figure 2 shows the temperature distribution around the outer surface of the rotary kiln. It can be seen that the temperature is highest on the wall, where it reaches 401 °C (674 K). It is noted that there is also a radial propagation of the temperature, which tends to decrease until it comes to the chosen ambient temperature of 5 °C (278 K).

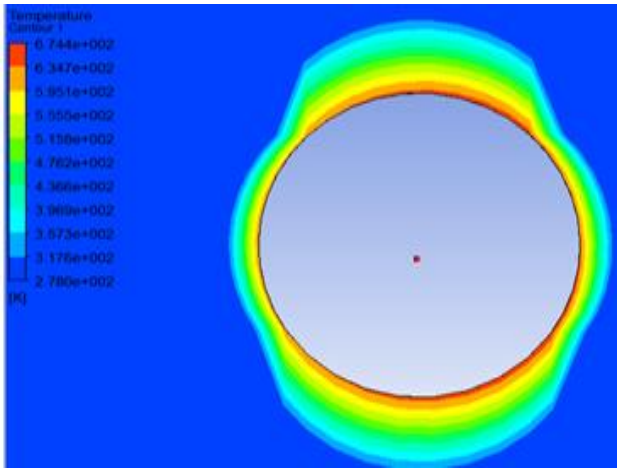

Fig. 2. Temperature contours

5.2.2 Velocity contour

Figure 3 shows the structure of the air velocity field around the shell of the rotary kiln. The flow velocity decreases to the point of stagnation, where it becomes zero. After this point, the velocity increases because of overpressure due to air contact with the shell, then it decelerates due to a negative pressure gradient.

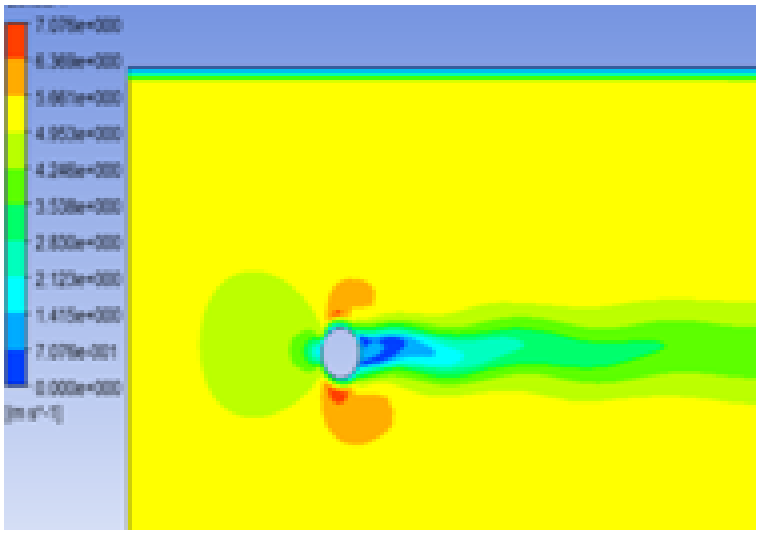

Fig. 3. Velocity contours

5.2.3 Pressure contour

Figure 4 shows the pressure distribution around the rotary kiln shell. It is found that the relative pressure is maximal at the stagnation point where it reaches 16.34 Pa; it then diminishes at the top and bottom of the shell, where it becomes almost zero. This is due to the fact that the air jet is deflected to the sides of the shell, to create zones of depression on either side of the shell.

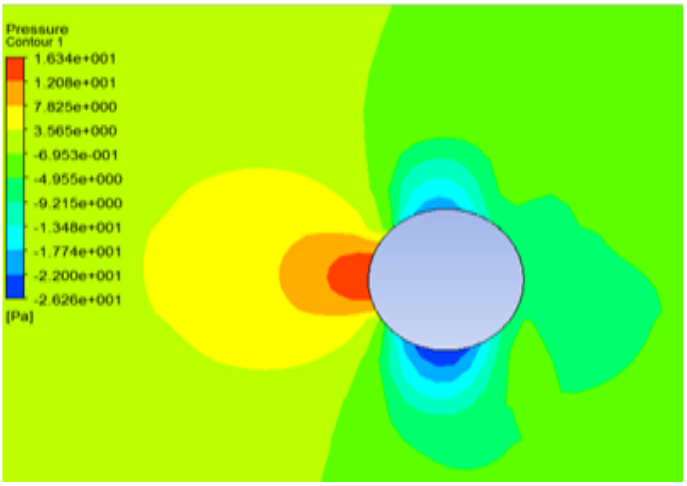

Fig. 4. Pressure contours

5.2.4 Variation of the injection air velocity

The rotary kiln is industrial equipment with an outdoor installation. Thus, it is stressed by air currents which can influence the behaviour of the temperature parameter. For this reason, we have taken this factor as a calculation parameter. We varied the air injection velocity from 5.86 m/s to 27.77 m/s. This velocity variation range is taken with respect to the actual conditions of an outdoor environment.

The aim of this case study is to determine the effect of the air injection velocity on the thermal behaviour of the shell. Four tests were carried out to deduce there from the maximum temperature value of the shell, as well as the Nusselt number.

Table 4 shows the evolution of the Nusselt number and shell temperature as a function of the air injection velocity. Note that the Nusselt number increases proportionally with the air injection velocity; it reaches the value of 8845 for an air injection velocity of 27.77 m/s. This is justified because the increase in velocity directly induces an increase in the Reynolds number, which results in an increase in the Nusselt number.

Table 4
Nusselt number and Shell temperature as a function of air injection velocity

Air velocity (m/s)	5.86	11.11	16.66	22.22	27.77
Number of Nusselt	4375	5503	6210	7360	8845
Shell temperature (°C)	401	330	298	274	255

This step consists in deducing the effect of this same parameter, namely the air injection velocity, on the maximum temperature of the shell. Also, Table 4 shows the evolution of the temperature of the shell. Note that the temperature decreases relatively as the air injection velocity increases.

We notice in this part that as the air injection velocity increases, the Nusselt number increases, with a decrease in the temperature of the shell, and thus favoring the cooling of the rotary kiln shell.

Figure 5 shows the variation in the temperature of the shell as a function of different values of the air injection velocity. We note that the shape of the curves corresponds well to the laminar regime characterized by the Poiseulle profile. The temperature increases to its maximum value near the shell, then it decreases to ambient temperature (5 °C) beyond the shell. For a high air injection velocity (27.77 m/s), cooling of the shell is observed, given that the temperature decreases from 401 °C to 255 °C, which corresponds to a 36 % rate of decline in temperature.

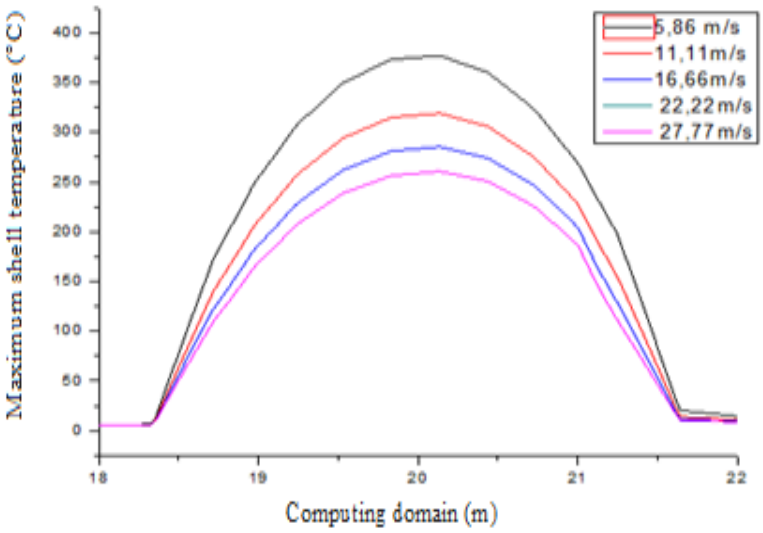

Fig. 5. Temperature of the shell as a function of the air injection velocity

5.2.5 Variation of the rotational velocity

The rotational velocity of the kiln was varied from 1 rpm to 5 rpm, in order to deduce the effect of this parameter on the temperature of the shell. The influence of the rotational velocity is due to the evolution of the Nusselt number and the maximum temperature of the shell.

Table 5 shows the variation of the Nusselt number and shell temperature as a function of the rotational velocity. For the chosen velocity range corresponding to that used in the process of a cement plant, the velocity does not have a great effect on the Nusselt number. Similarly, gives us the variation in the shell temperature as a function of the different rotation velocities. By increasing the rotational velocity from 1 rpm to 5 rpm, it causes an increase in the shell temperature by 8°C. This gap of minimal temperature justifies the coincidence of the temperature graph shown in Figure 6.

The rotary velocity of the kiln does not impact the evolution of the Nusselt number, it is noted that this maximum variation is around 1.3%. The same applies to the temperature of the shell, where the variation reaches a maximum value of 2%.

Table 5
Nusselt Number and Shell Temperature as a function of the rotational velocity

Rotary velocity (rpm)	1	2	3	4	5
Number of Nusselt	4343	4301	4285	4325	4299
Shell temperature (°C)	393	394	399	400	401

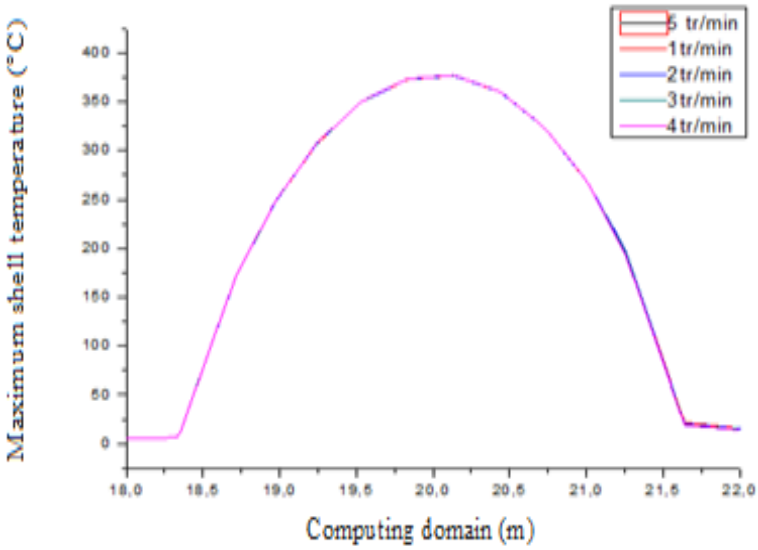

Fig. 6. The shell temperature as a function of the rotational velocity

5.2.6 Variation of the injection air temperature

In this section, we wanted to know the effect of the variation in ambient air temperature T_∞. For this purpose, we used the temperatures 5°C, 18 °C, 25 °C, and 40 °C. Figure 7 presents the variation in the temperature of the shell as a function of the temperature of the air. A rate of increase of 13% or 276 °C to 289 °C of the shell temperature is observed when the air temperature increases from 5 °C to 40 °C.

We note that this parameter, which is the temperature of the air injected into our kiln, does not have a great effect, because our equipment operates with very high temperatures compared to those of the air injected. The choice of air temperatures is dictated by the environment surrounding the kiln.

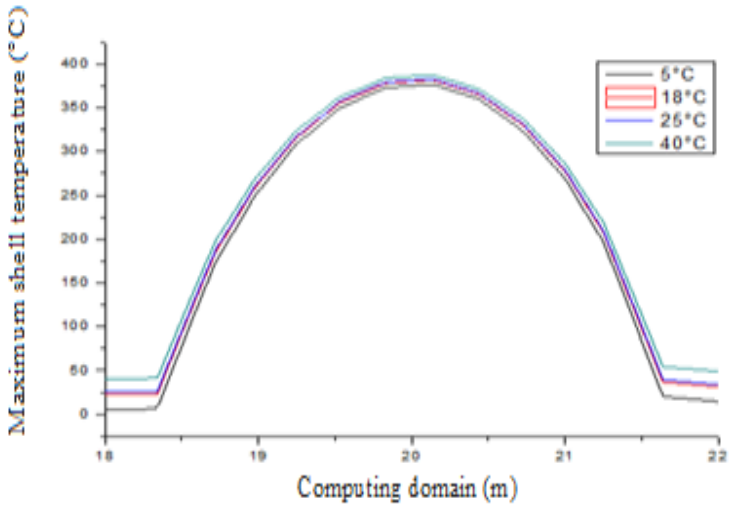

Fig. 7. Temperature of the ferrule as a function of the air temperature

5.3 2nd Case "Finned Cylinder"

The first section of our study showed us the presence of a very high-temperature gradient between the outer surface of the shell and its environment. The latter indicates the presence of a heat flow that must be released to allow the preservation in good condition of the rotary kiln shell. To this end, in this second part of our study, we wanted to install fins on the shell. This way, it is possible to increase the exchange surface and thus attempt to solve the problem of the heat flow release.

The geometric model has been reproduced, wherein the shell has four fins with l = 50mm long and e = 50mm wide. The boundary conditions are those used previously, namely that used by Mirhosseini *et al.,* [1] in his work, to deduce the effect of these fins on the shell temperature behaviour.

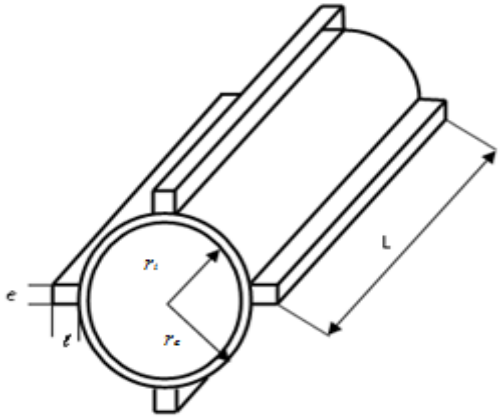

Fig. 8. Rotary kiln with four fins

5.3.1 Temperature distribution

Figure 9 shows the temperature distribution around the rotary kiln shell. With the insertion of the fins, we found that the temperature decreases to reach 164 °C (representing nearly half of the temperature of the smooth case). Also, we notice the presence of two vortices behind the two fins which are in a perpendicular position with respect to the flow. The presence of the fins gives rise to 2 vortices of different sizes.

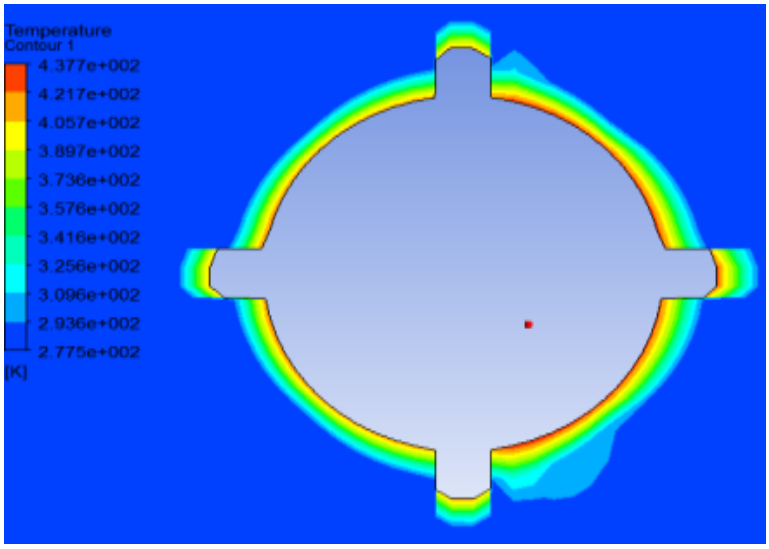

Fig. 9. The finned shell temperature

5.3.2 Variation of the air injection velocity

Under the same conditions as the case of the smooth shell, four tests were carried out to deduce the maximum value of the wall temperature, as well as the Nusselt number corresponding to each air injection velocity (Table 6). The results are shown in Table 6. The increase in the air injection velocity causes a slight decrease in the temperature of the finned shell, unlike the case of the smooth shell, where the temperature decreases considerably.

Table 6
Nusselt number and Temperature according to the air injection velocity

Air velocity (m/s)	5.86	11.11	16.66	22.22	27.77
Nusselt number	4375	5503	6210	7360	8845
Shell temperature (°C)	167.7	163.4	158.8	159	158

Figure 10 shows the variation in temperature of the finned shell as a function of different air injection velocities. The temperature profiles have the same tendency due to the position of the results extraction line. The temperature gradient when increasing the air injection velocity is not very significant (6 °C). Compared to the case without fins, we notice the presence at the top of the curve of a stable temperature with light fluctuations due to the presence of the fins. We note the presence of a flat at the level of the extremum of the curve, which is caused by the fin, creating a disturbance and also favouring an increase in temperature. The flats present at the level of the structure are essentially due to the disturbances created by the fins.

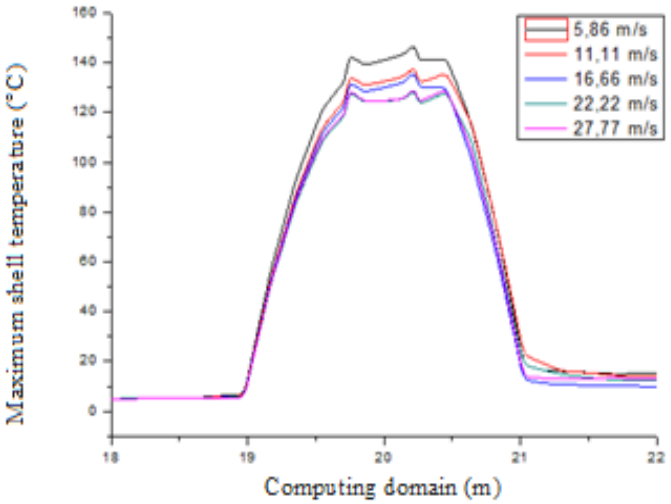

Fig. 10. Evolution of the temperature as a function of the air injection velocity

5.3.3 Rotational velocity variation

The rotational velocity of the kiln was varied from 1 rpm to 4 rpm to see its effect on the development of Nusselt number and the maximum temperature of the finned shell. For the same rotational velocities as those of the smooth case, the values of the Nusselt number are shown in Table 7 for the finned shell. As shown by the results in Table 7, as in the case of a smooth shell, the rotational velocity of the finned shell has no significant effect on the Nusselt number. For the same rotational velocities as those of the smooth case, the values of the shell temperature are shown. It should be noted that the best dissipation of the heat flow is located at a rotational velocity of 3 rpm with a value of the Nusselt number of 4446. As an instruction for the user of the kiln, the choice of this velocity is recommended, for better preservation of the equipment.

Table7
Nusselt number and Shell temperature as a function of the rotational velocity

Rotary velocity (rpm)	1	2	3	4	5
Nusselt number	4381	4490	4446	4148	4375
Temperature of shell (°C)	166.8	166	167.8	165.8	164.7

Figure 11 shows the variation in the temperature of the finned shell as a function of different rotational velocities. The temperature profiles have the same appearance. The temperature gradient when increasing the rotational velocity is not significant; it is approximately 3°C.

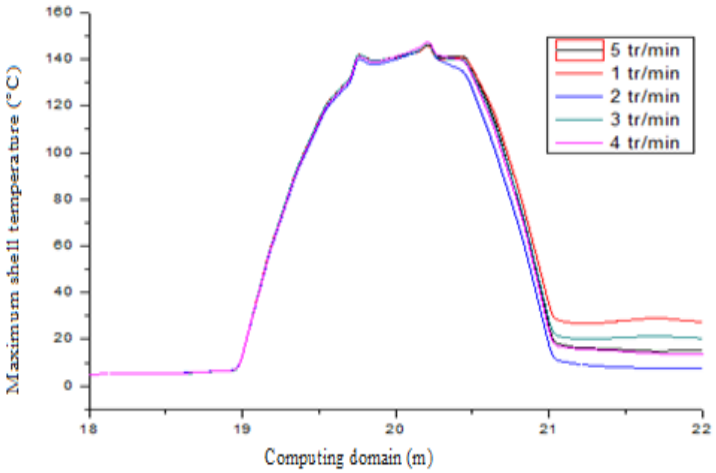

Fig. 11. Temperature evolution as a function of the rotational velocity

5.4 Comparison Between the Smooth Shell and the Finned Shell

To show the fins effect on the temperature of the kiln shell, a comparison was made between the two case studies (smooth and finned). Figure 12 shows the evolution of the temperature for the two cases. It is noted that the insertion of the fins causes a decrease in the maximum temperature for the finned shell. This decrease is about 36%, a decrease of the maximum temperature of 401 °C for the smooth shell to 164 °C for the finned shell. It is also noted that the increased temperature can only occur from 1 meter in length from the beginning of the shell, for the smooth case. While for the finned case, this only happens at 1.8 meters. This increase in distance is yielded by the decrease in temperature.

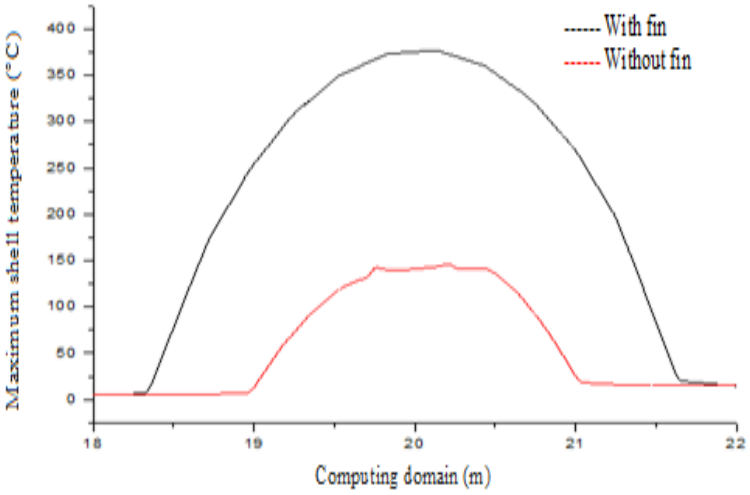

Fig. 12. The temperature evolution of the smooth and finned shells

Table 8 shows the Nusselt number values in the case of smooth and finned shells for a value of the rotary velocity of the kiln of 5 rpm. From the results, it can be said that the insertion of the fins causes an increase in the Nusselt number. This increase in the Nusselt number results in a significant exchange of the heat flow with the shell. Similarly, Table 9 and Table 10 summarize the drop in the

external temperature of the shell. This decrease is clearly visible for the 2 parameters, namely the rotary velocity and the air injection velocity on the kiln.

Table 8
Comparison of Nusselt number

Shells	Smooth	Finned
Nusselt Number	4299	4375

Table 9
Comparison of shell temperature as a function rotary velocity

	Rotary velocity (rpm)	1	2	3	4	5
case “smooth cylinder”	Shell temperature (°C)	393	394	399	400	401
case “finned cylinder”	Shell temperature (°C)	166.8	166	167.8	165.8	164.7

Table 10
Comparison of shell temperature as a function air velocity

	Air velocity (m/s)	5.86	11.11	16.66	22.22	27.77
case “smooth cylinder”	Shell temperature (°C)	401	330	298	274	255
case “finned cylinder”	Shell temperature (°C)	167.7	163.4	158.8	159	158

6. Conclusion

In this study, a numerical modelling was conducted by combining an unstructured mesh with the finite volume method. The solution was obtained by using the SIMPLE algorithm (pressure-velocity coupling).

The aim was to study the thermal behaviour of a rotary kiln shell. Two cases of numerical simulations were carried out. The first one consisted of simulating the rotary kiln section with the most significant thermal stress, namely the shell part where the external wall temperature was 500 °C. This shell was taken in this case as being smooth. In the second case, the same simulations were reproduced with the same boundary conditions, with additional fins inserted to the outer surface of the shell.

The results showed that the increase in Nusselt number and the decrease in temperature were a function of the air injection velocity for both cases. For a smooth shell, the rate of decrease was 36% by increasing the air injection velocity. While for a finned shell, the decrease was 41.82%.

Regarding the kiln rotational velocity, the same observation was made in both cases, namely a slight increase in Nusselt number and a slight decrease in the temperature of the outer surface of the shell. Although for the case of a finned shell, there was a better result compared to the case without fins.

Overall, the predominant parameter for the shell cooling is the air injection velocity for both geometric configurations. More significant cooling may be obtained when the shell is equipped with fins.

References

[1] Mirhosseini, Mojtaba, Alireza Rezaniakolaei, and Lasse Rosendahl. "Numerical study on heat transfer to an arc absorber designed for a waste heat recovery system around a cement kiln." *Energies* 11, no. 3 (2018): 671. https://doi.org/10.3390/en11030671

[2] Shahin, Hamed, Saeid Hassanpour, and Ahmad Saboonchi. "Thermal energy analysis of a lime production process: Rotary kiln, preheater and cooler." *Energy Conversion and Management* 114 (2016): 110-121. https://doi.org/10.1016/j.enconman.2016.02.017

[3] Atmaca, Adem, and Recep Yumrutaş. "Analysis of the parameters affecting energy consumption of a rotary kiln in cement industry." *Applied Thermal Engineering* 66, no. 1-2 (2014): 435-444. https://doi.org/10.1016/j.applthermaleng.2014.02.038
[4] Acharya, Swastik, and Sukanta K. Dash. "Natural convection heat transfer from a short or long, solid or hollow horizontal cylinder suspended in air or placed on ground." *Journal of Heat Transfer* 139, no. 7 (2017). https://doi.org/10.1115/1.4035919
[5] Gaurav, Gajendra Kumar, and Shabina Khanam. "Analysis of temperature profile and% metallization in rotary kiln of sponge iron process through CFD." *Journal of the Taiwan Institute of Chemical Engineers* 63 (2016): 473-481. https://doi.org/10.1016/j.jtice.2016.02.035
[6] Liu, Hong, Hongchao Yin, Ming Zhang, Maozhao Xie, and Xi Xi. "Numerical simulation of particle motion and heat transfer in a rotary kiln." *Powder Technology* 287 (2016): 239-247. https://doi.org/10.1016/j.powtec.2015.10.007
[7] Li, Gongfa, Ze Liu, Guozhang Jiang, Honghai Liu, and Hegen Xiong. "Numerical simulation of the influence factors for rotary kiln in temperature field and stress field and the structure optimization." *Advances in Mechanical Engineering* 7, no. 6 (2015): 1687814015589667. https://doi.org/10.1177/1687814015589667
[8] Sak, C., R. Liu, DS-K. Ting, and G. W. Rankin. "The role of turbulence length scale and turbulence intensity on forced convection from a heated horizontal circular cylinder." *Experimental thermal and fluid science* 31, no. 4 (2007): 279-289. https://doi.org/10.1016/j.expthermflusci.2006.04.007
[9] Sanitjai, Surachai, and Richard J. Goldstein. "Forced convection heat transfer from a circular cylinder in crossflow to air and liquids." *International journal of heat and mass transfer* 47, no. 22 (2004): 4795-4805. https://doi.org/10.1016/j.ijheatmasstransfer.2004.05.012
[10] Nakamura, Hajime, and Tamotsu Igarashi. "Variation of Nusselt number with flow regimes behind a circular cylinder for Reynolds numbers from 70 to 30 000." *International journal of heat and mass transfer* 47, no. 23 (2004): 5169-5173. https://doi.org/10.1016/j.ijheatmasstransfer.2004.05.034
[11] Scholten, J. W., and D. B. Murray. "Unsteady heat transfer and velocity of a cylinder in cross flow—I. Low freestream turbulence." *International journal of heat and mass transfer* 41, no. 10 (1998): 1139-1148. https://doi.org/10.1016/S0017-9310(97)00250-0
[12] Zukauskas, Ai, and J. Ziugzda. "Heat transfer of a cylinder in crossflow." *Washington* (1985).
[13] Sarma, T. S., and S. P. Sukhatme. "Local heat transfer from a horizontal cylinder to air in cross flow: influence of free convection and free stream turbulence." *International Journal of Heat and Mass Transfer* 20, no. 1 (1977): 51-56. https://doi.org/10.1016/0017-9310(77)90083-7
[14] Jain, P. C., and B. S. Goel. "A numerical study of unsteady laminar forced convection from a circular cylinder." (1976): 303-307. https://doi.org/10.1115/1.3450537
[15] Schmidt, Ernst, and Karl Wenner. "Heat transfer over the circumference of a heated cylinder in transverse flow." *Forschung auf dem Gebiete des Ingenieurwesens* 12, no. NACA-TM-1050 (1943).
[16] Elfaghi, Abdulhafid MA, Alhadi A. Abosbaia, Munir FA Alkbir, and Abdoulhdi AB Omran. "CFD Simulation of Forced Convection Heat Transfer Enhancement in Pipe Using Al2O3/Water Nanofluid." *Journal of Advanced Research in Numerical Heat Transfer* 8, no. 1 (2022): 44-49. https://doi.org/10.37934/cfdl.14.9.118124
[17] Kanafiah, Siti Farah Haryatie Mohd, Abdul Rahman Mohd Kasim, Syazwani Mohd Zokri, and Mohd Rijal Ilias. "Combined Convective Transport of Brinkman-viscoelastic Fluid Across Horizontal Circular Cylinder with Convective Boundary Condition." *Journal of Advanced Research in Fluid Mechanics and Thermal Sciences* 89, no. 2 (2022): 15-24. https://doi.org/10.37934/arfmts.89.2.1524
[18] Shafie, Sharidan, Rahimah Mahat, and Fatihhi Januddi. "Numerical Solutions of Mixed Convection Flow Past a Horizontal Circular Cylinder with Viscous Dissipation in Viscoelastic Nanofluid." *Journal of Advanced Research in Micro and Nano Engineering* 1, no. 1 (2020): 24-37.
[19] Mujumdar, Kaustubh S., K. V. Ganesh, Sarita B. Kulkarni, and Vivek V. Ranade. "Rotary Cement Kiln Simulator (RoCKS): Integrated modeling of pre-heater, calciner, kiln and clinker cooler." *Chemical Engineering Science* 62, no. 9 (2007): 2590-2607. https://doi.org/10.1016/j.ces.2007.01.063
[20] Mujumdar, K. S., and V. V. Ranade. "Simulation of rotary cement kilns using a one-dimensional model." *Chemical engineering research and design* 84, no. 3 (2006): 165-177. https://doi.org/10.1205/cherd.04193
[21] Patankar, Suhas V. *Numerical heat transfer and fluid flow*. CRC press, 2018. https://doi.org/10.1201/9781482234213
[22] Menter, Florianr. "Zonal two equation kw turbulence models for aerodynamic flows." In *23rd fluid dynamics, plasmadynamics, and lasers conference*, p. 2906. 1993. https://doi.org/10.2514/6.1993-2906
[23] Incropera, Frank P., David P. DeWitt, Theodore L. Bergman, and Adrienne S. Lavine. *Fundamentals of heat and mass transfer*. Vol. 6. New York: Wiley, 1996.

[24] Kim, Hyun Jung, Byoung Hoon An, Jinil Park, and Dong-Kwon Kim. "Experimental study on natural convection heat transfer from horizontal cylinders with longitudinal plate fins." *Journal of Mechanical Science and Technology* 27 (2013): 593-599. https://doi.org/10.1007/s12206-012-1236-3